the plant journal

SEB Society for Experimental Biology

The Plant Journal (2016) **86,** 161–174 doi: 10.1111/tpj.13158

The anaphase-promoting complex initiates zygote division in Arabidopsis through degradation of cyclin B1

Lei Guo[1,2,†], Li Jiang[1,†,‡], Ying Zhang[1], Xiu-Li Lu[1], Qi Xie[3], Dolf Weijers[4] and Chun-Ming Liu[1,*]

[1]*Key Laboratory of Plant Molecular Physiology, Institute of Botany, Chinese Academy of Sciences, Beijing 100093, China,*

[2]*University of Chinese Academy of Sciences, Beijing 100049, China,*

[3]*Institute of Genetics and Developmental Biology, Chinese Academy of Sciences, Beijing 100101, China, and*

[4]*Laboratory of Biochemistry, Wageningen University, Dreijenlaan 3, 6703 HA, Wageningen, The Netherlands*

Received 19 November 2015; revised 27 February 2016; accepted 1 March 2016; published online 8 March 2016.

*For correspondence (e-mail cmliu@ibcas.ac.cn).

†These two authors contributed equally to this work.

‡Present address: Chinese Academy of Fishery Science, Beijing 100141, China.

SUMMARY

As the start of a new life cycle, activation of the first division of the zygote is a critical event in both plants and animals. Because the zygote in plants is difficult to access, our understanding of how this process is achieved remains poor. Here we report genetic and cell biological analyses of the *zygote-arrest 1* (*zyg1*) mutant in Arabidopsis, which showed zygote-lethal and over-accumulation of cyclin B1 D-box-GUS in ovules. Map-based cloning showed that *ZYG1* encodes the anaphase-promoting complex/cyclosome (APC/C) subunit 11 (APC11). Live-cell imaging studies showed that *APC11* is expressed in both egg and sperm cells, in zygotes and during early embryogenesis. Using a *GFP-APC11* fusion construct that fully complements *zyg1*, we showed that *GFP-APC11* expression persisted throughout the mitotic cell cycle, and localized to cell plates during cytokinesis. Expression of non-degradable cyclin B1 in the zygote, or mutations of either *APC1* or *APC4*, also led to a *zyg1*-like phenotype. Biochemical studies showed that APC11 has self-ubiquitination activity and is able to ubiquitinate cyclin B1 and promote degradation of cyclin B1. These results together suggest that APC/C-mediated degradation of cyclin B1 in Arabidopsis is critical for initiating the first division of the zygote.

Keywords: APC11, cyclosome, zygote activation, cell cycle, ubiquitination, *Arabidopsis thaliana*.

INTRODUCTION

In sexual organisms, the initiation of zygote division is the first step in embryogenesis, which marks the starting point of a new life cycle. In animals, fertilization often triggers an acute oscillation of cytosolic Ca^{2+} in the zygote, followed by elimination of maternal mRNAs and proteins, and expression of zygotic genes to start embryogenesis (Wassarman, 1987; Baroux *et al.*, 2008; Horner and Wolfner, 2008). Fulfillment of these sequential events requires both paternal and maternal factors (Sette *et al.*, 1997; Saunders *et al.*, 2002; Baroux *et al.*, 2008). Plant embryogenesis involves successive events including zygote elongation and division, tissue differentiation and organogenesis (De Smet *et al.*, 2010). Live-cell imaging in Arabidopsis has shown the presence of cytoplasmic Ca^{2+} signatures during double fertilization (Denninger *et al.*, 2014). Genetic studies carried out in Arabidopsis have led to the identification of many genes that are essential for embryogenesis (Meinke *et al.*, 2008; De Smet *et al.*, 2010). Among them, *EMBRYONIC FACTOR 1* (*FAC1*) that encodes an AMP deaminase and *ZEUS* that encodes a thymidylate kinase are essential for the first division of the zygote (Xu *et al.*, 2005; Ronceret *et al.*, 2008). In addition, mutations of a DNA ligase (Andreuzza *et al.*, 2010), *YAO1*, that encodes a nucleolar protein (Li *et al.*, 2010), *AtCDC5* (Lin *et al.*, 2007) or *Cullin 1* (Shen *et al.*, 2002) also showed partial arrest at the zygote stage, suggesting the importance of cell cycle genes in zygote divisions.

At the transcriptional level, the extent to which the expression of maternal and paternal genomes contributes to early zygotic embryogenesis is still under debate. Some studies have shown that paternal and maternal genomes are transcriptionally equivalent in early zygotic embryogenesis (Nodine and Bartel, 2012), while others have shown that the maternal genome is transcriptionally dominant (Autran *et al.*, 2011; Del Toro-De León *et al.*, 2014).

In this study, we took a genetic approach in *Arabidopsis thaliana* to identify genes that are critical for the initiation of zygote division. The *zygote-arrest 1* (*zyg1*) mutant reported here showed phenotypes of zygote-lethal and over-accumulation of CYCB1;1D-box-GUS in arrested ovules, suggesting a role of *ZYG1* in promoting cell cycle progression. Map-based cloning revealed that *ZYG1* encodes subunit 11 (APC11) of the anaphase-promoting complex/cyclosome (APC/C), a ubiquitin ligase that is known to target cyclins and securins for destruction (Peters, 2006). Biochemical studies have shown that APC11 is able to ubiquitinate cyclin B1;1, leading to degradation of cyclin B1;1. In addition, mutations in two other APC/C subunits, *APC1* or *APC4*, or expression of a non-degradable cyclin B1;1 under an embryo-specific *DD45* promoter, also showed a similar zygote-lethal phenotype.

RESULTS

Isolation of the zygote-lethal *zyg1* mutant

Forty additional zygote-lethal mutants were identified by differential interference contrast (DIC) microscopy examination of embryo-lethal ovules from a population of approximately 5000 *A. thaliana* (Col-0) M_2 plants mutagenized by ethyl methanesulfonate (EMS) treatment as described in Xu *et al.* (2005). In these mutants at least a fraction of embryos were arrested at the single-cell zygote stage. Since homozygous ovules are lethal, all these mutants were maintained in a heterozygous state. After backcrossing to Col-0 for at least three generations, detailed phenotypic analyses were performed in these mutants. The *zyg1* mutant was notable as it exhibited a cell cycle arrest phenotype (see below). In aborted *zyg1* ovules, 46.0% showed developmental arrest of the embryo at the single-cell zygote stage (n = 463), while others continued to one to three cycles of cell division before abortion. These arrested zygotes were mostly elongated and had visible cell walls (Figure 1b; indicated by an open arrowhead).

Genetic analyses showed that 25.5% of the ovules (n = 353) in *zyg1*/+ siliques were aborted, suggesting that the *zyg1* phenotype is caused by a single-gene recessive mutation, and the presence of either a maternal or a paternal *ZYG1* allele is sufficient to initiate zygote division. Reciprocal crosses between *zyg1*/+ and Col-0 showed that transmission through the male was reduced slightly while through the female it was reduced significantly, especially in *zyg1-2* (Table 1), indicating that *ZYG1* plays a role in both microsporogenesis and megasporogenesis.

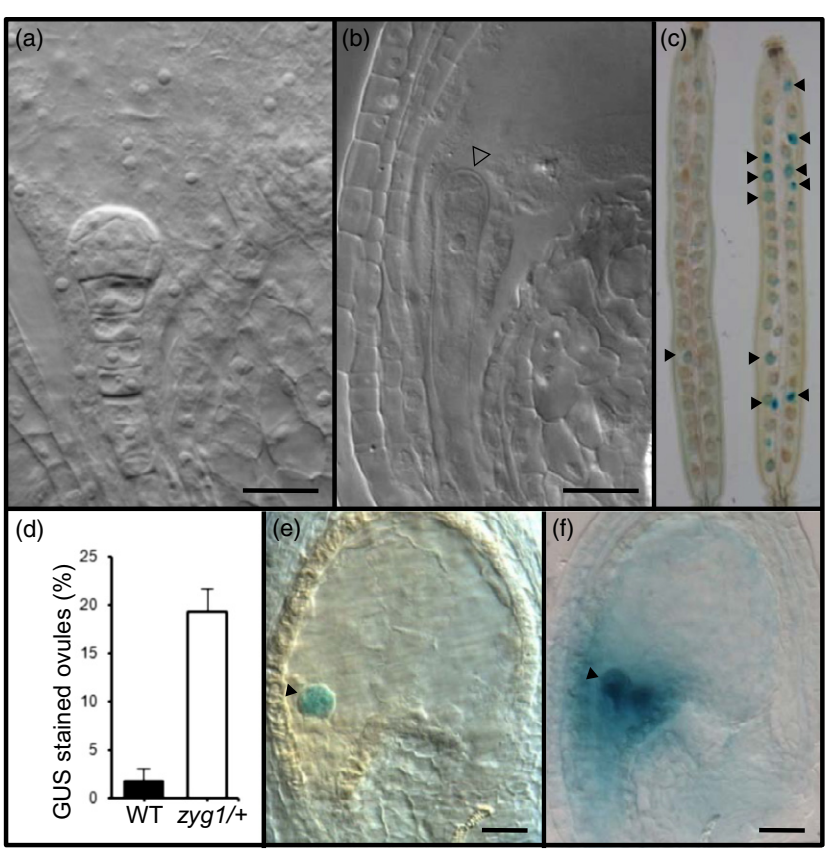

Figure 1. The *zyg1* mutant exhibits zygote-lethal and CYCB1;1D-box-GUS over-accumulation phenotypes.
(a), (b) Differential interference contrast (DIC) microscopy images showing the arrested zygote (b; indicated by an open arrowhead) in *zyg1*, compared with the wild-type embryo at the same stage (a). (c) Accumulation of GUS in ovules (arrowheads) in a silique from *zyg1*/+ carrying a homozygous *CYCB1;1D-box-uidA* transgene (right), compared with a silique from the wild type carrying the same construct (left). (d) Frequencies of GUS-positive ovules in siliques from the wild type (WT) and *zyg1/+* plants carrying a homozygous *CYCB1;1D-box-uidA* transgene. (e), (f) Strong GUS staining observed in an arrested *zyg1* zygote (f; arrowhead) compared with weak GUS staining in the wild-type embryo (e; arrowhead) in the same silique from a *zyg1*/+ plant carrying a homozygous *CYCB1;1D-box-uidA* transgene. Bars = 30 μm.

Table 1 Transmission efficiencies of the maternal and paternal *zyg1* alleles

Cross combinations		Progeny plants examined			
Female	Male	Wild type	Heterozygous	Transmission frequencies (%)	*P*-values
zyg1-1/+	Col-0	215	140	78.9	5.6×10^{-6}
Col-0	*zyg1-1*/+	131	116	93.9	6.6×10^{-3}
zyg1-2/+	Col-0	130	50	55.6	5.9×10^{-7}
Col-0	*zyg1-2*/+	70	56	88.9	3.3×10^{-3}

The *P*-value represents the probabilities for unbiased 100% transmissions. $P < 0.05$ indicates that the transmission efficiency was compromised.

zyg1 showed early cell cycle arrest and cyclin hyperaccumulation phenotypes

To characterize the defects in *zyg1*, we introduced the *CYCB1;1D-box-uidA* [cyclin B1;1 destruction box (D-box) fused with a β-glucuronidase (GUS; gene *uidA*)] reporter construct (Colón-Carmona *et al.*, 1999) to *zyg1*/+ by crossing. As reported before, the CYCB1;1D-box-GUS fusion protein is subjected to degradation at the cell cycle transition from metaphase to anaphase, and thus cells with GUS staining are about to exit mitosis (Colón-Carmona *et al.*, 1999). The GUS activity in ovules excised from *zyg1/+* plants carrying a homozygous *CYCB1;1D-box-uidA* transgene was assessed. Results showed that, in the wild-type plants, GUS staining was only observed in 1.8% of ovules ($n > 200$) collected when embryos were at the pre-globular stage. However, GUS staining was observed in 19.3% ($n > 200$) of arrested *zyg1* ovules examined at the same stage (Figure 1c,d). In addition, GUS staining in arrested *zyg1* ovules was more intense than in the wild type (Figure 1e,f). Such a CYCB1;1D-box-GUS over-accumulation phenotype was observed in aborted ovules from *zyg1*/+ (94.4%, $n = 72$; Figure 1f) but rarely in wild-type-looking ones in the same silique (2.5% $n = 204$; Figure 1e). These results suggest a cell cycle defect in defective *zyg1* ovules.

ZYG1 encodes the APC11 subunit of the APC/C

Using a population of approximately 2000 F_2 plants obtained from a cross between *zyg1*/+ (Col-0) and a plant of the Landsberg *erecta* (L*er*) ecotype, *ZYG1* was mapped to a 96-kb interval on chromosome 3. We screened T-DNA insertion lines of all 31 annotated genes in this region and found that *Salk_019654*, with a T-DNA inserted into the second intron of the annotated *At3g05870* (Figure 2a), showed a similar zygote-lethal phenotype as *zyg1*. We sequenced the genomic region of the gene in *zyg1*/+ and identified a G to A point mutation that converted a highly conserved cysteine (C) residue to tyrosine (Y) (Figure 2b). Reciprocal crosses between *zyg1*/+ and *Salk_019654* failed to complement the mutant phenotype in the F_1 generation, indicating that these two mutations are allelic. Accordingly, *zyg1* and *Salk_019654* were re-named *zyg1-1* and *zyg1-2*, respectively.

After sequencing the *ZYG1* transcript from cDNA prepared from the wild-type Arabidopsis seedlings, we found that the intron–exon structure prediction for *APC11* in the TAIR and GenBank databases was inaccurate, with the presence of a single-nucleotide exon missing and the inclusion of a 9-bp intronic sequence in the cDNA (Figure S1 in the Supporting Information; Guo and Liu, 2015). As illustrated in Figure 2(a), the corrected *ZYG1* gene encodes a 252-bp transcript, producing an 84-amino-acid (aa) polypeptide that showed high sequence similarity to APC11 proteins from rice (OsAPC11), maize (ZmAPC11), *Physcomitrella patens* (PpAPC11), human (HsAPC11), zebrafish (DrAPC11) and *Talaromyces marneffei* (TmAPC11) (Capron *et al.*, 2003a; Figure 2b). *APC11* is a single gene in the Arabidopsis genome, which shares 36% sequence identity at the amino acid level with AtRBX1, a component in the Skp1/Cullin/F-box (SCF) protein complex (Figure 2b; Gray *et al.*, 2002; Lechner *et al.*, 2002).

To confirm if the mutation in *APC11* is responsible for the *zyg1* phenotype, we generated *pAPC11:GFP-APC11:tAPC11* and *pAPC11:APC11-GFP:tAPC11* constructs, with the green fluorescence protein gene (*GFP*) inserted in-frame, respectively, to the N- or C-terminus of the *APC11* coding region. The *APC11* fragment used consists of 1506-bp 5′ upstream (*pAPC11*), 839-bp coding and 648-bp 3′ downstream sequences (*tAPC11*). These constructs were transformed to the wild-type *A. thaliana* (Col-0). Several single-insertion lines with detectable *GFP* expression were obtained and crossed to *zyg1-1*/+ plants. Among the F_2 progenies obtained, we identified homozygous *zyg1-1*/*zyg1-1* plants carrying either *pAPC11:GFP-APC11:tAPC11* or *pAPC11:APC11-GFP:tAPC11.* Detailed examination of these plants revealed neither zygote- nor embryo-lethal phenotypes, suggesting that these fusion constructs are functional and able to complement the *zyg1-1* phenotype.

Bi-allelic expression of *APC11* during embryogenesis

To access the expression of *ZYG1*, transgenic plants carrying either *pAPC11:APC11-GFP:tAPC11* or *pAPC11:*

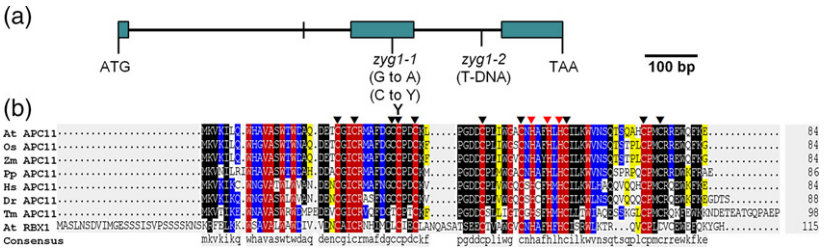

Figure 2. *APC11* gene structure and sequence alignment.
(a) The structure of the *APC11* gene. Note that in *zyg1-1* a G to A mutation in the third exon led to a C to Y conversion at the amino acid level, and in *zyg1-2* a T-DNA was inserted into the third intron.
(b) Alignment of APC11 from Arabidopsis (At), rice (Os), maize (Zm), *Physcomitrella patens* (Pp), human (Hs), zebrafish (Dr) and *Talaromyces marneffei* (Tm), and RBX1 from Arabidopsis. Identical amino acids are shown in red, while similar amino acids are in black, blue or yellow based on their conservation levels. The C to Y change in *zyg1-1* is labeled. Conserved C residues are indicated by black arrowheads, and histidine (H) by red arrowheads.

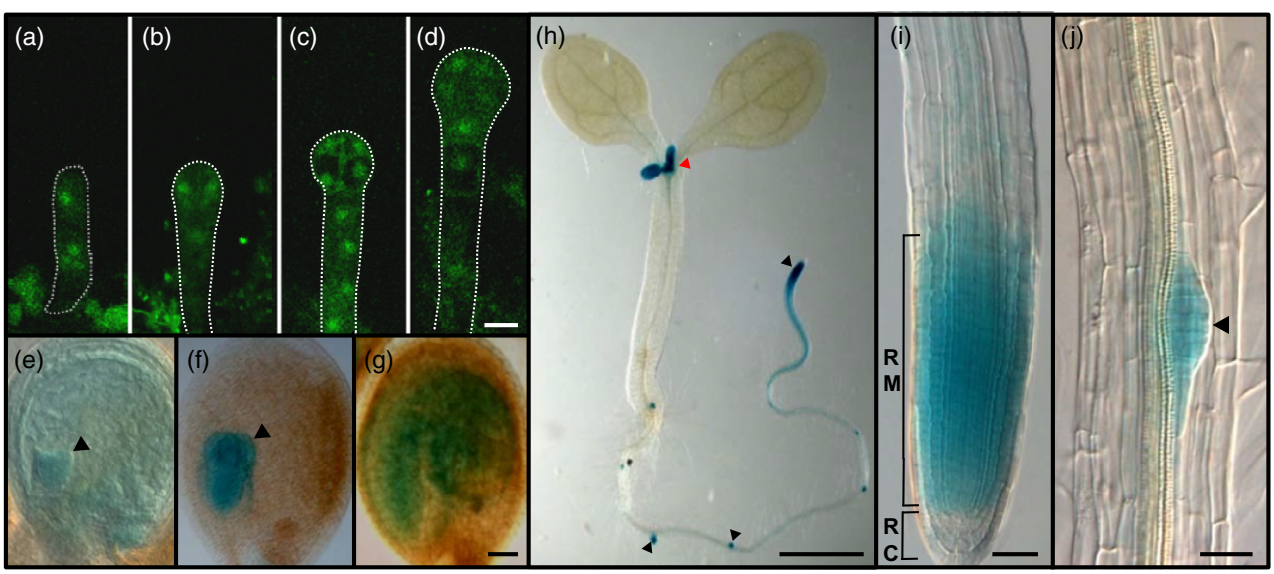

Figure 3. The expression pattern of *APC11*.
(a)–(d) In *pAPC11:APC11-GFP:tAPC11* complemented *zyg1-1/zyg1-1* plants, *GFP* expression was observed in both the embryo proper and the suspensor in pro-embryos. Bar in (d) = 10 μm for (a)–(d). (e)–(g) *uidA* expression was detected in heart-shaped (e), torpedo (f) and cotyledonary stage embryos (g) in a transgenic plant carrying *pAPC11:APC11-uidA:tAPC11*. Embryos are indicated by black arrowheads. Bar in (g) = 30 μm for (e)–(g). (h) At the seedling stage, *uidA* expression was detected in shoot apices (indicated by red arrowheads) and root tips (indicated by black arrowheads) in transgenic plants carrying *pAPC11:APC11-uidA:tAPC11*. Bar = 1 mm. (i), (j) In roots of transgenic plant carrying *pAPC11:APC11-uidA:tAPC11*, *uidA* expression was observed in the root meristem (i; indicated by RM) and the lateral root primodium (j; arrowhead), but not in the elongation zone, the quiescent center and the root cap (i; indicated by RC). Bar in (i) = 30 μm; bar in (j) = 50 μm.

APC11-uidA:tAPC11 (made by replacing the *GFP* gene in *pAPC11:APC11-GFP:tAPC11* with *uidA*) were examined. As shown in Figure 3, *ZYG1* expression was observed in embryos at all stages examined (Figure 3a–g), while *uidA* expression in the endosperm was restricted to early stage ovules and declined when embryos reached the torpedo stage (Figure 3e–g). During vegetative growth, *uidA* expression was observed in all meristematic tissues examined, in particular shoot and root apices (Figure 3h,i) and lateral root primordia (Figure 3j; indicated by an arrowhead). Confocal microscopic examination showed that in *pAPC11:APC11-GFP:tAPC11* transgenic plants *GFP* expression was observed in both embryo proper and suspensor cells (Figure 3a–d). Within these cells, the GFP signal was present in both the nucleus and cytoplasm (Figure 3a–d), as reported previously (Roodbarkelari *et al.*, 2010).

To define *APC11* expression more accurately, we replaced the *GFP* in *pAPC11:APC11-GFP:tAPC11* with a nucleus-localized *SV40-3×GFP*, to produce *pAPC11:APC11-SV40-3×GFP:tAPC11*. Transformation and progeny analyses showed that the *pAPC11:APC11-SV40-3×GFP:tAPC11* construct is also able to complement the *zyg1-1* mutant, producing wild-type-appearing plants in the *zyg1-1/zyg1-1* background. In these transgenic plants, *GFP* expression

was detected from the tetrad stage to mature microspores during microsporogenesis (Figure 4a–e). In mature and germinating pollen, *GFP* expression was only observed in sperm cells (Figure 4d,e; indicated by red arrowheads) and barely in the vegetative nucleus (indicated by a white arrowhead). During megasporogenesis, *GFP* expression was continuously observed from megaspore mother cells to the mature embryo sac (Figure 4h–m).

To access the expression of *APC11* during double fertilization, *pAPC11:APC11-SV40-3×GFP:tAPC11* transgenic plants were used to pollinate transgenic plants carrying egg-cell-specific *pEC1:H2B-RFP* (Ingouff *et al.*, 2009). Under a confocal microscope, we observed the release of GFP-labeled sperm (Figure 4n–p; indicated with 's') into the embryo sac at 5 h after pollination (HAP). At a slightly later stage (approximately 6 HAP), fusion of the red fluorescent protein (RFP)-labeled egg cell with GFP-labeled sperm was observed, producing a zygote with both green and red fluorescence (Figure 4q–s; indicated with 'z'). Concurrently, the fusion of non-labeled central nucleus with the other GFP-labeled sperm led to the formation of a nucleus with green fluorescence (Figure 4q–s; indicated with 'c').

The Mendelian segregation of the recessive *zyg1* phenotype suggests that both maternal and paternal *APC11* alleles are active in zygotes. To confirm this at the transcriptional level, reciprocal crosses between homozygous *pAPC11:APC11-SV40-3×GFP:tAPC11* and the wild-type (Col-0) plants showed that, indeed, *GFP* expression was observed in both the zygote and the central nucleus immediately after fertilization, no matter whether the transgenic plant was used as male or female parent (Figure 5a, d; endosperm nuclei, white arrowheads). When examined at about 8 HAP with pollens from *pAPC11:APC11-SV40-3×GFP:tAPC11* plants, 78.6% (n = 94) zygotes showed GFP fluorescence. Similarly, when *pAPC11:APC11-SV40-3×GFP:tAPC11* plants were pollinated with wild-type pollen and examined in the same manner, a similar ratio of GFP-positive zygotes (76.2%, n = 106) was observed. Considering the variations in fertilization time in different ovules and the detectability of the GFP signal, we believe that *APC11* is expressed in zygotes immediately after fertilization.

APC11 is localized to the cell plate during cytokinesis

It has been shown that several APC/C proteins exhibit dynamic changes in localization during the cell cycle (Blilou *et al.*, 2002; Capron *et al.*, 2003b; Fülöp *et al.*, 2005; Pérez-Pérez *et al.*, 2008; Eloy *et al.*, 2011; Wang *et al.*, 2012). To find out if this is the case for APC11, we crossed *mCherry-TUA5* transgenic plants (Gutierrez *et al.*, 2009) with *pAPC11:GFP-APC11:tAPC11* plants. mCherry-TUA5 decorated cytoskeletal configurations (Figure 6a′–e′) such as cortical microtubules (Figure 6a′), pre-prophase band (Figure 6b′), mitotic spindle (Figure 6c′) and phragmoplast (Figure 6d′,e′) in root meristematic cells. We observed that in cells at the interphase (Figure 6a), prophase (Figure 6b) and metaphase (Figure 6c), GFP-APC11 fluorescence was distributed in both the cytosol and nucleus, as reported previously (Roodbarkelari *et al.*, 2010). However, during anaphase and telophase, in addition to the cytosolic localization, GFP-APC11 was observed in the mid-plane of the forming cell plate (Figure 6d,e; indicated by red arrowheads), indicating a role of APC11 in cytokinesis.

APC11 has self-polyubiquitination activity

To address if APC11 has E3 ligase activity, an *in vitro* ubiquitination assay was performed. A glutathione *S*-transferase-tagged *APC11* (*GST-APC11*) construct was made and transformed to *Escherichia coli* to purify the GST-APC11, and the GST without APC11 was produced and purified as a control. When GST-APC11 was incubated *in vitro* with His-tagged ubiquitin-activating enzyme E1 (His-E1) from wheat, His-tagged ubiquitin conjugating enzyme E2 (His-E2) from human and His-tagged ubiquitin 14 (His-Ub) from Arabidopsis (Zhao *et al.*, 2013), polyubiquitination of APC11 was observed after 30-min incubations and detected with either anti-His (Figure 7a) or anti-GST (Figure 7b) antibodies (right panels, indicated by arrowheads). Such a polyubiquitination was not observed in the control reaction with GST (Figure 7a,b; left panels). The polyubiquitination was saturated after 60 min, as the number and intensity of those ubiquitination bands did not increase further when the incubation time was extended (Figure 7a,b; right panels). These polyubiquitination bands were not observed when either His-E1, His-E2, His-Ub or GST-APC11 was omitted from the reaction (Figure 7c,d; indicated by arrowheads), no matter what anti-His (Figure 7c) or anti-GST antibodies (Figure 7d) were used. These results suggest that, in the presence of E1, E2 and ubiquitin, APC11 is able to execute self-polyubiquitination.

APC11 ubiquitinated cyclin B1;1 and promoted cyclin B1;1 degradation

We next addressed whether the Arabidopsis APC11 is able to ubiquitinate and promote cyclin B1;1 degradation. A *His-CYCB1;1-Myc* construct was made, with the *cyclin B1;1* cDNA from Arabidopsis fused with a N-terminal His-tag and a C-terminal 4×Myc-tag, and transformed to *E. coli*. A His-CYCB1;1-Myc fusion protein was purified using a Ni-agarose column. An *in vitro* ubiquitination assay was performed using His-E1, His-E2, His-Ub, His-CYCB1;1-Myc and GST-APC11. Polyubiquitination of the His-CYCB1;1-Myc was detected using an anti-Myc antibody after incubation for 90 min (Figure 7e; right panel), and the intensity of these polyubiquitination bands was increased when the incubation time was extended to 120 min, while no polyubiquitination was detected when GST-APC11 was replaced by GST (Figure 7e; left panel). These results suggest that APC11 is able to ubiquitinate cyclin B1;1.

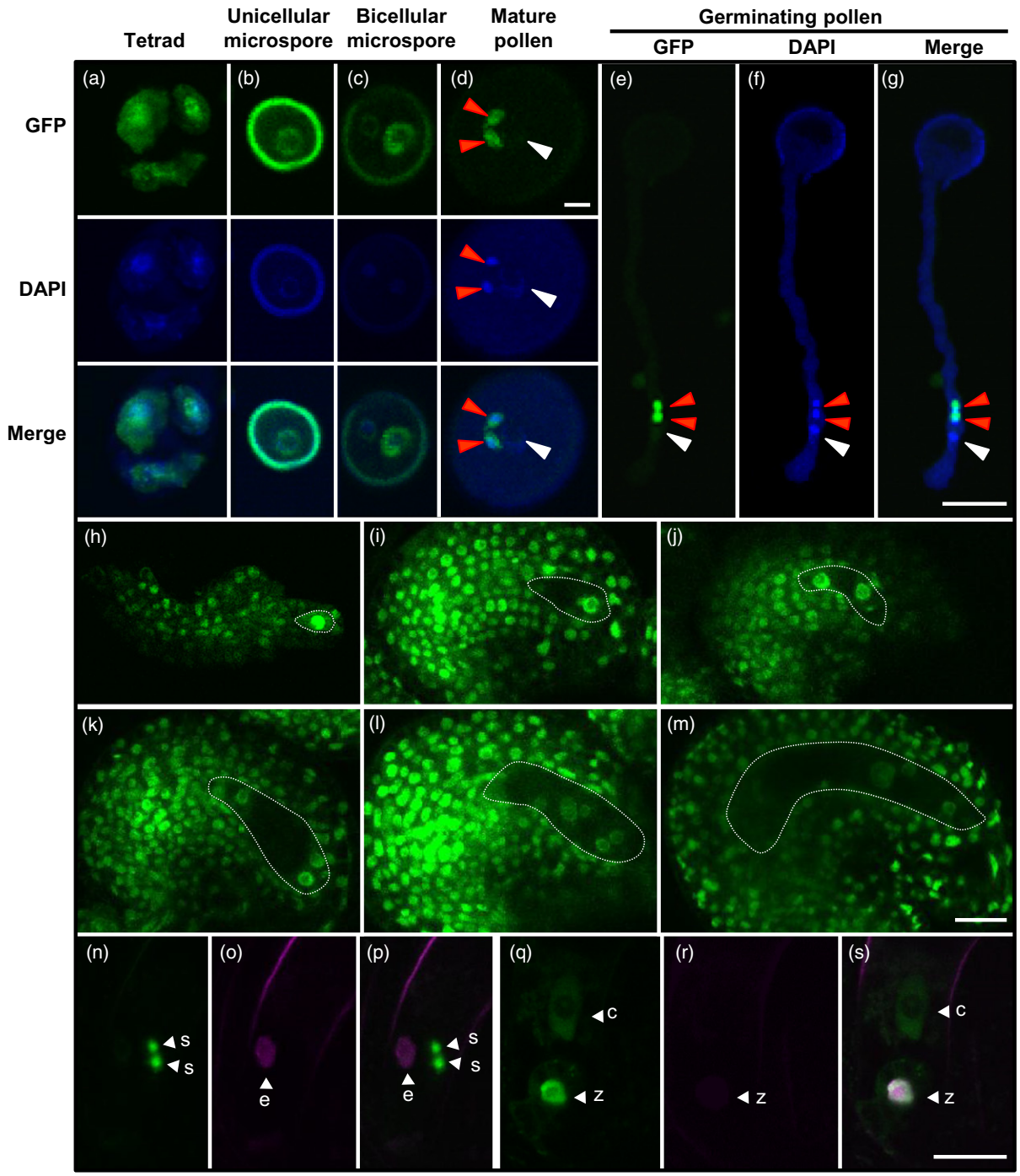

Figure 4. *APC11* expression during gametogenesis and fertilization.
(a)–(d) In transgenic plants carrying a homozygous *pAPC11:APC11-SV40-3*× *GFP:tAPC11*, *GFP* expression (top panel) was observed primarily in nuclei of tetrad (a), unicellular (b) and bicellular stage microspores (c), and in sperm cells (red arrowheads) in a mature pollen (d). Nuclei were showed by 2-(4-amidinophenyl)-6-indolecarbamidine dihydrochloride (DAPI) staining (middle panel), and merged pictures were showed in the bottom panel. Note that no GFP was detected in the vegetative nucleus (d; white arrowhead) of mature pollen. Bar in (d) = 5 μm for (a)–(d). (e)–(g) *GFP* expression in sperm cells (e; red arrowheads) of a germinating pollen grain from transgenic *zyg1-1*/*zyg1-1* plants carrying *pAPC11:APC11-SV40-3*× *GFP:tAPC11*, while absent in the vegetative nucleus (f; white arrowhead). The merged image of GFP and DAPI staining is showed in (g). Bar in (g) = 20 μm for (e)–(g). (h)–(m) *GFP* expression in megaspore mother cell (h), one-nucleate (i), two-nucleate (j), four-nucleate (k) and seven-celled (l) and mature ovules (m) in transgenic *zyg1*/*zyg1* plants carrying *pAPC11:APC11-SV40-3*× *GFP:tAPC11*, showing continuous *APC11* expression during megasporogenesis. Bar in (m) = 20 μm for (h)–(m). (n)–(p) Arrival of sperm ('s' in n and p) in the embryo sac, but not yet fused with the egg cell ('e' in o and p), observed in ovules from a transgenic plant carrying *pEC1:H2B-RFP*, 5 h after pollination with pollen from a plant carrying *pAPC11:APC11-SV40-3*× *GFP:tAPC11*. Note that at this stage two sperm cells (s) have not yet fused with the egg. (q)–(s) Both GFP (q) and RFP (r) were detected in the zygote ('z' in q–s) after the double fertilization, while only GFP was detected in the central nucleus ('c' in q and s). Bar in (s) = 20 μm for (n)–(s).

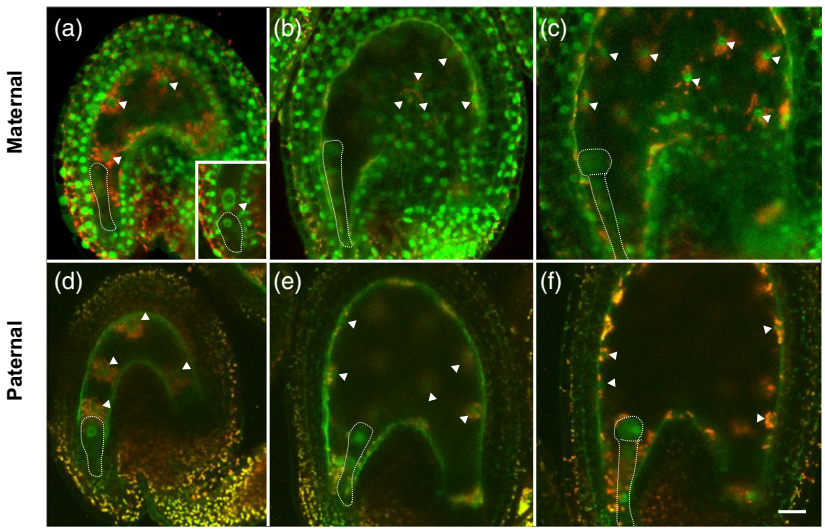

Figure 5. Bi-allelic *APC11* expression in zygotes, embryos and endosperm.
Transgenic plants carrying *pAPC11:APC11-SV40-3×GFP:tAPC11* were used as female (a)–(c) or male (d)–(f) to cross with the wild type. Note that in both crosses the GFP signals were observed in the zygote right after fertilization (inset in a), elongated zygotes (a, d), embryos (b, c, e, f), and endosperm (a–f; white arrowheads). The autofluorescence (red) is included to show the general structure of the ovules. Dotted lines are used to trace the zygotes and pro-embryos. Bar in (f) = 20 μm for (a)–(f).

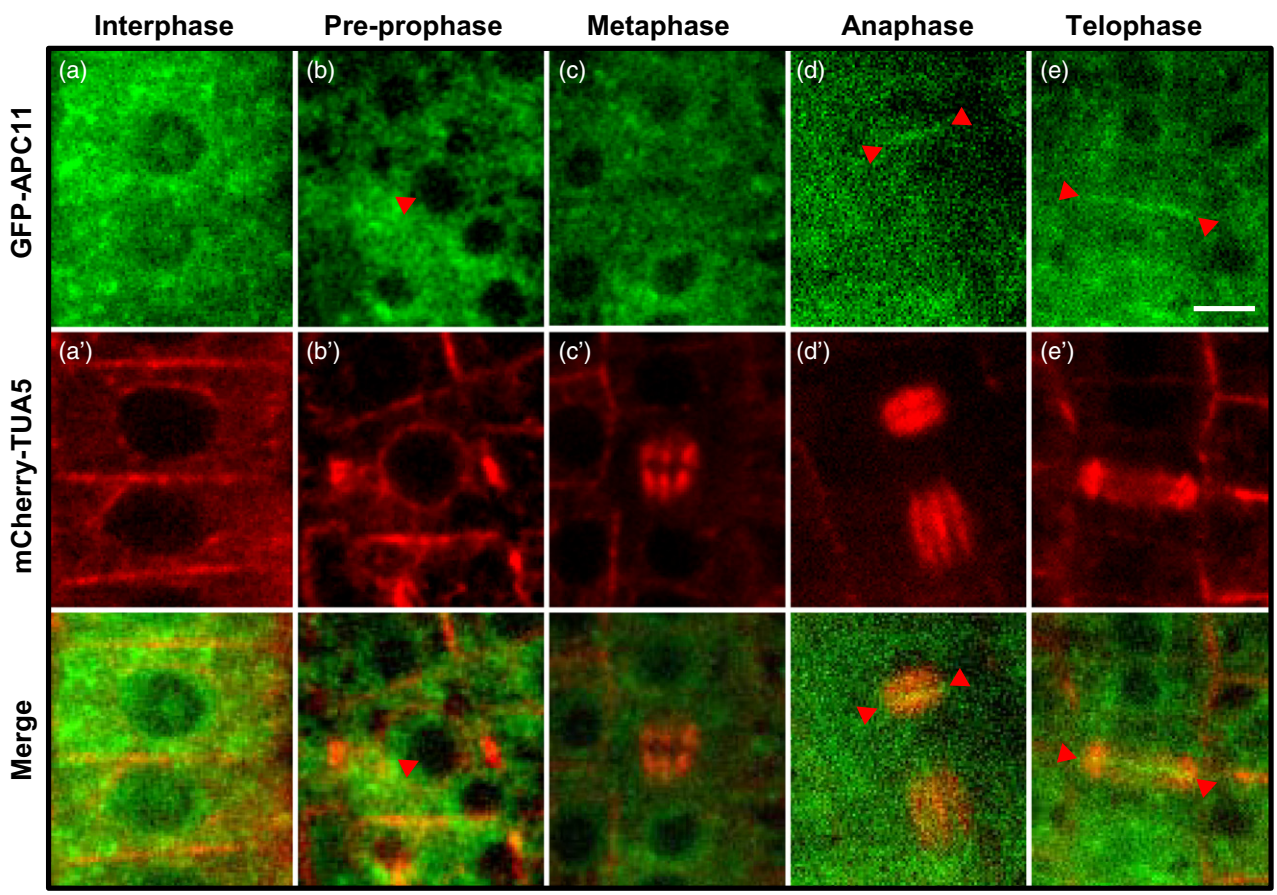

Figure 6. Subcellular localization of APC11 during mitosis.
In 4-day-old transgenic plants carrying both *pAPC11:GFP-APC11:tAPC11* and *mCherry-TUA5*, GFP fluorescence was observed in both cytosol and nuclei in cells at the interphase (a), pre-prophase (b), and metaphase (c), while in anaphase (d) and telophase cells (e), in addition to cytosol, the GFP signal was also observed in phragmoplasts (red arrowheads). mCherry-TUA5 fluorescence (a′–e′) was used to indicate different phases of the cell cycle. The merged images are showed at the bottom. Bar in (e) = 10 μm for (a)–(e).

We then addressed whether APC11 promotes degradation of cyclin B1;1. Constructs of *p35S:GFP-APC11* and *p35S:CYCB1;1-Myc*, expressed under the CaMV 35S promoter, were made and transformed individually to *Nicotiana benthamiana* leaves by infiltrations (Liu *et al.*, 2010). The GFP-APC11 and CYCB1;1-Myc proteins extracted from

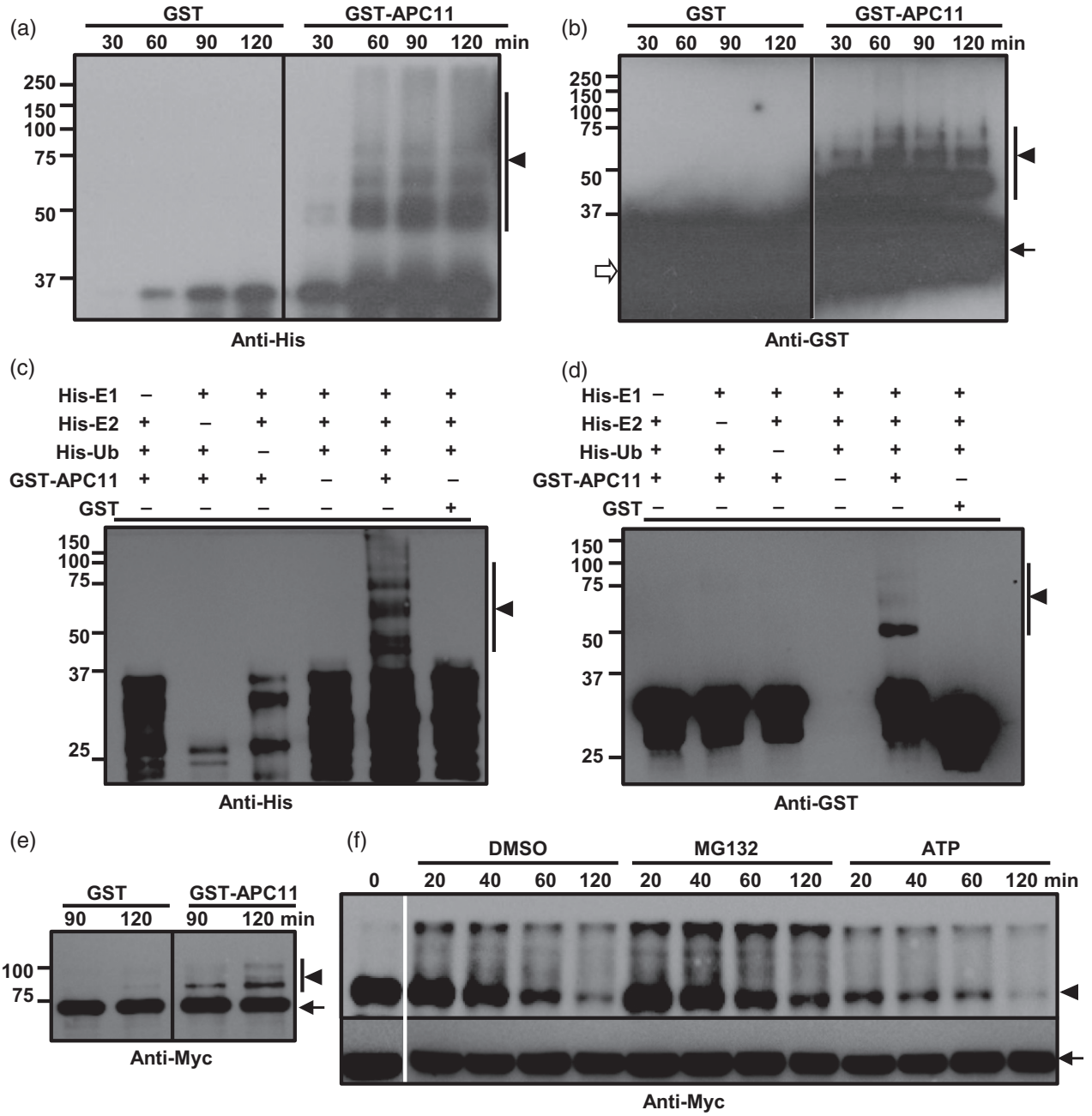

Figure 7. APC11 ubiquitinated and promoted degradation of cyclin B1;1.
(a), (b) GST-APC11 self-ubiquitination was detected using anti-His (a) or anti-GST (b) antibodies when GST-APC11 was incubated with His-E1, His-E2 and His-Ub at 24°C for 30, 60, 90 or 120 min. No ubiquitination was observed when GST was used. GST-APC11 polyubiquitination bands are indicated by arrowheads, GST by an open arrow and GST-APC11 by an arrow. (c), (d) APC11 polyubiquitination (arrowheads) requires His-E1, His-E2 and His-Ub, as detected using anti-His (c) or anti-GST (d) antibodies. Note that no polyubiquitination was detected when His-E1, His-E2 or His-Ub was omitted. (e) Polyubiquitination (arrowhead) of His-CYCB1;1-Myc (arrow) was detected after incubation with GST-APC11, His-E1, His-E2 and His-Ub at 24°C for 90 or 120 min, but not when GST was used. (f) APC11 promotes degradation of cyclin B1;1. CYCB1;1-Myc was incubated with GFP-APC11 in the presence of either DMSO, MG132 or ATP for different times at 24°C, and the CYCB1;1-Myc degradation (arrowhead) was detected by an anti-Myc antibody. Note the increased or decreased CYCB1;1-Myc degradation when ATP or MG132 was applied, respectively, as compared with DMSO as a control. The actin (arrow) level, shown by an anti-actin antibody, was used as a loading control.

these leaves were mixed and the stability of CYCB1;1-Myc was monitored by Western blot using an anti-Myc antibody. We observed that, in the presence of ATP, the CYCB1;1-Myc protein (Figure 7f; indicated by an arrowhead) was rapidly degraded in a time-dependent manner. In contrast, when MG132, a 26S proteasome inhibitor, was added, the CYCB1;1-Myc protein was much more stable (Figure 7f). Although such degradation was also observed

in the control treatment when ATP was replaced by dimethyl sulfoxide (DMSO), it was much slower than the reaction with ATP (Figure 7f). These results suggest that APC11 is able to ubiquitinate cyclin B1;1 to promote degradation of cyclin B1;1.

Expression of *cyclin B1;1* with a mutated D-box in embryos led to a zygote-lethal phenotype

To address whether the zygote-lethal phenotype in *zyg1* was caused by over-accumulation of cyclin B1;1, we changed the D-box in cyclin B1;1 from RQVLGDIGN to AQVAGDIGN through PCR-based site-directed mutagenesis to generate *CYCB1;1*$^{\triangle D\text{-}box}$, with a *uidA* reporter gene fused to its C-terminus. It has been shown that cyclin B1 with a mutated D-box is much more stable (Weingartner *et al.*, 2004). The *pDD45:CYCB1;1*$^{\triangle D\text{-}box}$*-uidA* fusion construct made using an embryo-specific promoter *pDD45* that is active from the zygote stage onwards (Steffen *et al.*, 2007) was transformed to *A. thaliana* (Col-0) using the floral dip method (Clough and Bent, 1998). The *pDD45:CYCB1;1-uidA* construct with the native cyclin B1;1 was made and transformed to *A. thaliana* (Col-0) as a control. Phenotypic analyses of T_1 transgenic plants carrying *pDD45:CYCB1;1*$^{\triangle D\text{-}box}$*-uidA* showed that, among 22 lines examined, six displayed an embryo-lethal phenotype. Further analyses in one of these lines under a DIC microscope revealed that 26.6% of ovules ($n > 200$) in siliques carried embryos arrested at the zygote stage, and 38.3% were at the two- to eight-cell stages. The zygote-lethal phenotype, with zygote elongation, resembled the *zyg1* mutant. As a control, no such phenotype was observed in any of these lines among the 33 independent transgenic lines carrying *pDD45:CYCB1;1-uidA* that were examined (Figure 8c). The GUS assay revealed that strong GUS signals were consistently observed in ovules from plants carrying *pDD45:CYCB1;1*$^{\triangle D\text{-}box}$*-uidA* ($n > 200$; Figure 8b), while only weak GUS staining was occasionally observed in ovules from *pDD45:CYCB1;1-uidA* plants (Figure 8a). The strong GUS staining is mostly observed in those small ovules from *pDD45:CYCB1;1*$^{\triangle D\text{-}box}$*-uidA* transgenic plants with a zygote-lethal phenotype (Figure 8b), suggesting that compromised degradation of CYCB1;1$^{\triangle D\text{-}box}$-GUS may have caused the zygote-lethal phenotype.

Mutations in *APC1* or *APC4* also showed a zygote-lethal phenotype

To find out if the zygote-lethal phenotype in *zyg1* was caused by a general defect in APC/C, we re-examined ovules from *apc1-1*/+ and *apc4-3*/+. These mutants have been reported previously with defective female gametogenesis and embryogenesis but not a zygote-lethal phenotype (Wang *et al.*, 2012, 2013). When ovules ($n = 306$) from of *apc1-1*/+ were cleared and examined under a DIC microscope 24.8% showed a female gamete defect and 15.7% were embryo-lethal; among these 22.9% were aborted at the zygote stage (Figure 8f; Table S1). Similarly, 28.6% of ovules ($n = 238$) were aborted before fertilization and 17.2% showed embryo-lethality; of these 24.4% were arrested at the zygote stage (Figure 8g; Table S1). These zygote-lethal phenotypes were indistinguishable from that of *zyg1*.

DISCUSSION

The first division of the zygote is a critical event in all sexual organisms. Through combined genetic, cell biological and biochemical studies we have shown in this study that APC/C-mediated degradation of cyclin B1 is essential for the first division of the zygote in Arabidopsis.

The essential role of APC/C in the initiation of zygote division

The 14-subunit APC/C complex is an E3 ubiquitin ligase that is conserved among all eukaryotic organisms (Chang and Barford, 2014). It is known that APC/C acts together with its activators CDC20 or CDH1 to degrade cyclins and securins, leading to irreversible progression of the cell cycle (Peters, 2006). In *Xenopus*, the activity of APC/C in the egg is inhibited by Early Mitotic Inhibitor 2 (Emi2), and the degradation of the Emi2 in response to Ca^{2+} oscillations releases the inhibition of APC/C and consequently triggers the division of the zygote (Schmidt *et al.*, 2005; Tung *et al.*, 2005; Tischer *et al.*, 2012). In plants, several APC/C subunits have been shown to be critical for gametogenesis and embryogenesis (Capron *et al.*, 2003b; Kwee and Sundaresan, 2003; Pérez-Pérez *et al.*, 2008; Eloy *et al.*, 2011; Zheng *et al.*, 2011; Wang *et al.*, 2012, 2013), while the role of APC/C in zygote division has not been shown. In this study we showed that mutations of *APC11* led to zygote-lethal and cyclin B1 over-accumulation phenotypes. Through re-examination of the *apc1-1*/+ and *apc4-3*/+ mutants reported previously (Wang *et al.*, 2012, 2013), we observed that mutations of *APC1* or *APC4* also led to a similar zygote-lethal phenotype, suggesting the critical role of APC/C in initiating zygote division.

Although a large number of genes involved in mitosis and cytokinesis have been identified in plants (Boruc and Van Damme, 2015; Müller and Jürgens, 2015), the direct link between these two successive processes is not yet known. In this study we observed that at the anaphase and telophase of the mitotic cell cycle, the GFP-APC11 fusion protein is localized to the mid-plane of the forming cell plate. This is striking, suggesting a role for APC11 in linking mitosis and cytokinesis. However, since the *pAPC11:APC11-SV40-3*×*GFP:tAPC11* construct (with the APC11 fused to a nuclear localization signal) is able to complement *zyg1*, the extent of the contribution of APC11 to mitosis and cytokinesis remains to be investigated.

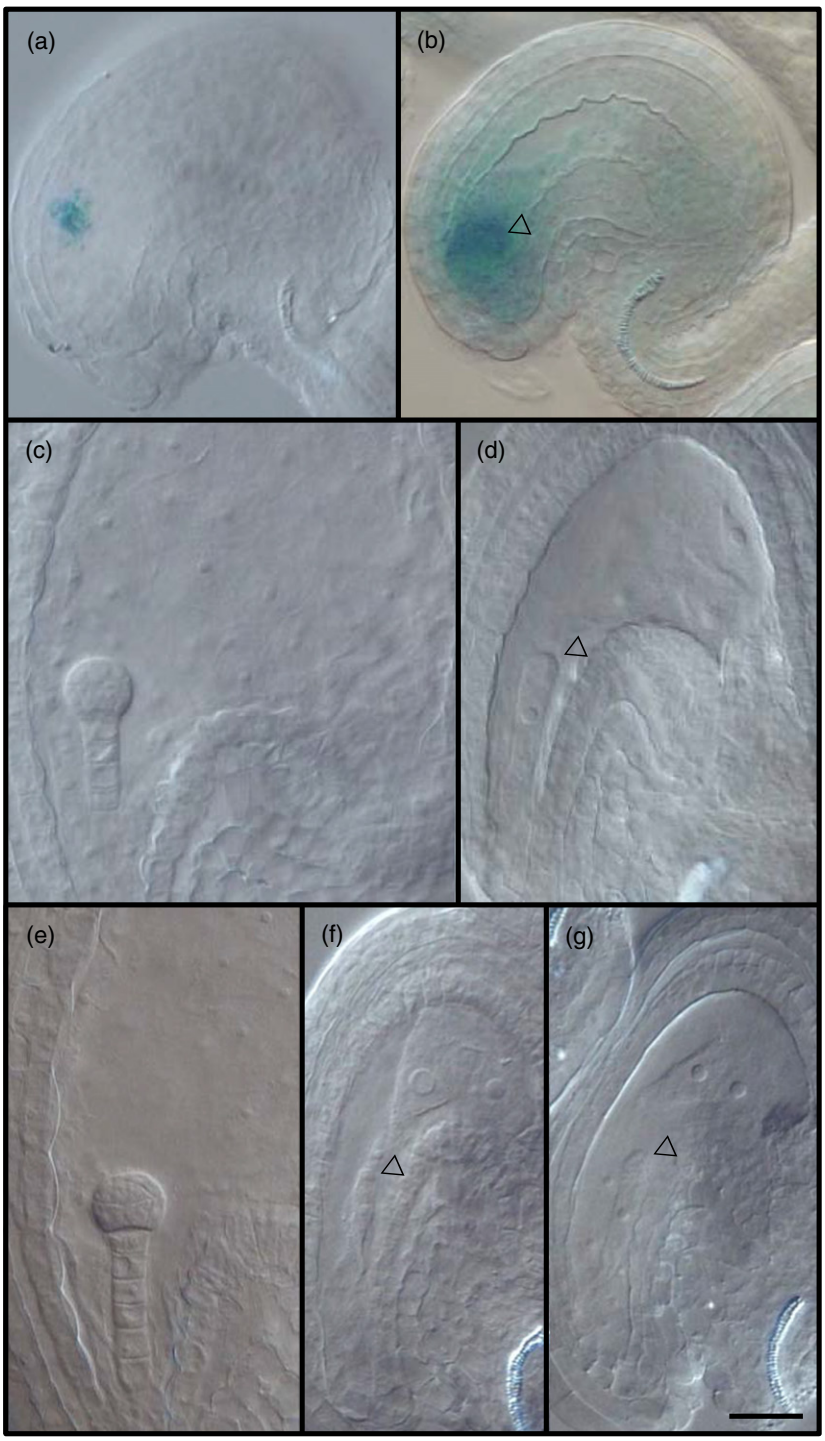

Figure 8. *pDD45:CYCB1;1*$^{\Delta D\text{-}box}$*-uidA* transgenic plants, and *apc1-1* or *apc4-3* mutant showed zygote-lethal phenotype.
(a), (b) Enhanced *uidA* expression was detected in ovules from transgenic plants carrying *pDD45:CYCB1;1*$^{\Delta D\text{-}box}$*-uidA* (b) and not from those carrying *pDD45:CYCB1;1-uidA* (a). (c), (d) Transgenic plants carrying *pDD45:CYCB1;1* $^{\Delta D\text{-}box}$*-uidA* showed a zygote-lethal phenotype (d; open arrowhead) compared with the wild-type one from *pDD45:CYCB1;1-uidA* transgenic plant (c). (e)–(g) Zygote-lethal phenotype observed in ovules from *apc1-1*/+ (f) or *apc4-3*/+ plants (g), compared with the wild-type one (e). Bar in (g) = 20 μm for all photos.

Maternal-to-zygotic transition in Arabidopsis

The Mendelian segregation of the *zyg1* phenotype implies that the presence of either a maternal or a paternal *APC11* allele is sufficient for the initiation of zygote division. Consistently, data from expression analyses using the *pAPC11:APC11-SV40-3*×*GFP:tAPC11* construct that is able to complement *zyg1-1* defects showed that *APC11* is expressed in both egg and sperm cells before fertilization, and throughout early embryo and endosperm development. The expression of *APC11* during microsporgenesis and megasporogenesis also explains why reduced transmission occurs in both males and females when heterozygous *zyg1*/+ plants were reciprocally crossed with the wild type,

implying that a fraction of gametes was defective in development before fertilization, as observed in several mutants in other APC/C subunit genes (Capron *et al.*, 2003b; Kwee and Sundaresan, 2003; Pérez-Pérez *et al.*, 2008; Eloy *et al.*, 2011; Zheng *et al.*, 2011; Wang *et al.*, 2012, 2013). Bi-allelic *APC11* expression was observed in zygotes and throughout early embryogenesis, which is in consistent with the proposition that both maternal and paternal *APC11* alleles contribute to the zygote division in Arabidopsis. Since the APC11-SV40-3×GFP fusion protein might be different from the endogenous APC11 protein in its stability, we could not exclude absolutely the possibility that the GFP signal we detected may come, or partially come, from carryover expressions from the sperm and egg cells.

Maternal-to-zygotic transition is an important process in animals that usually occurs several cell cycles after fertilization (Baroux *et al.*, 2008). The zygotic cleavage in sea urchin relies on maternally stored products, and the expression of the zygotic genome is not required until the larvae metamorphose (Baroux *et al.*, 2008). However, it is unknown whether maternal-to-zygotic transition is involved in plant embryogenesis. It is of interest to note that only a few genes are known so far to be essential for zygote division in animals (Raich *et al.*, 1998; Wu *et al.*, 2003), while in plants mutations of a handful of genes showed zygote-lethal phenotypes (Shen *et al.*, 2002; Xu *et al.*, 2005; Lin *et al.*, 2007; Ronceret *et al.*, 2008; Andreuzza *et al.*, 2010; Li *et al.*, 2010). In this study we identified *ZAG1* as a gene that is essential for zygote division, and *ZAG1* is expressed in zygotes immediately after fertilization. Together with the expressions observed in *AtRPS5A* and *FAC1* (Weijers *et al.*, 2001; Xu *et al.*, 2005), we speculate that in plants bi-allelic activation occurs at least in a fraction of the genome right after fertilization.

Several reports showed that maternal transcripts are dominant in early embryos (Vielle-Calzada *et al.*, 2000; Autran *et al.*, 2011; Del Toro-De León *et al.*, 2014), while others showed that maternal and paternal alleles contribute equally in early embryo development (Nodine and Bartel, 2012; Yu *et al.*, 2012). A recent genetic and cell biological study performed in a set of 49 embryo-lethal mutants showed that although most genes tested showed bi-allelic expression, delayed paternal gene expression was observed in some of those genes (Del Toro-De León *et al.*, 2014). Our present study seems to support a mode of equal paternal and maternal contributions in early embryogenesis.

APC11 ubiquitinates cyclin B1 and promotes cyclin B1 degradation

The CYCB1;1D-box-GUS over-accumulation phenotype in *zyg1-1* ovules suggests that APC11 may function in promoting degradation of cyclin B1. This proposition is supported by the observations that the *zyg1*-like phenotype was observed in transgenic plants when *cyclin B1;1* with a mutated D-box was expressed under the embryo-specific *DD45* promoter (Steffen *et al.*, 2007). These results imply that APC11 may function to degrade cyclin B1, which then triggers the division of the zygote.

In animals it has been shown that APC11 is able to execute self-ubiquitination, and to ubiquitinate and degrade securin *in vitro* in the presence of E1 and E2 enzymes (Gmachl *et al.*, 2000; Leverson *et al.*, 2000). Biochemical studies performed in this study illustrated that the APC11 in Arabidopsis is also able to execute self-ubiquitination *in vitro* in the presence of E1 and E2, suggesting that APC11 is the catalytic subunit of the APC/C complex. Furthermore, we demonstrated *in vitro* that APC11 is able to polyubiquitinate cyclin B1;1, promoting degradation of cyclin B1;1 in a 26S proteasome-dependent manner. It is apparent that timely degradation of cyclin B1;1 through APC/C-mediated polyubiquitination is critical for initiating zygote division in Arabidopsis. Of course how the APC/C itself is activated upon fertilization, and if a similar Emi2 degradation machinery is present in plants, remain to be studied.

EXPERIMENTAL PROCEDURES

Plant material and growth conditions

Plants of *A. thaliana*, ecotypes Col-0 and L*er*, were grown at 21°C in a growth room with 16-h light (100 μmol photons m^{-2} sec^{-1}) per day. A T-DNA insertion line, *Salk_019654* (Col-0), was obtained from the Nottingham Arabidopsis Stock Centre (http://arabidopsis.info/). For mutagenesis, Col-0 seeds were treated with EMS (Sigma, http://www.sigmaaldrich.com/) and screened for putative zygote-lethal mutants in M_2 plants as described (Xu *et al.*, 2005).

Genetic analysis and map-based cloning

zyg1-1/+ was backcrossed to Col-0 for three generations before further analyses were carried out. For transmission analyses, the number of *zyg1-1*/+ and wild-type progeny were counted in BC_1 populations after reciprocal crosses. The transmission frequency was calculated as the number of heterozygous plants/50% (total number of BC_1 plants). Map-based cloning was performed in 2000 F_2 progeny from a cross between *zyg1-1*/+ and L*er*. A point mutation was detected after sequencing candidate genes in a *zyg1-1*/+ plant.

Molecular cloning

For complementation and expression analyses, three constructs, *pAPC11:GFP-APC11:tAPC11*, *pAPC11:APC11-GFP:tAPC11* and *pAPC11:APC11-uidA:tAPC11*, were made using the full-length *APC11* genomic sequence consisting of 1506-bp 5′ upstream, 839-bp coding region and 648-bp 3′ downstream sequences, with a *GFP* and *uidA* in-frame fused to the N- or C-terminus of *APC11*, respectively. *pAPC11:APC11-SV40-3×GFP:tAPC11* was made by replacing the *GFP* in *pAPC11:APC11-GFP:tAPC11* with the *SV40-3×GFP* (De Rybel *et al.*, 2011). These constructs were introduced to Arabidopsis (Col-0) by *Agrobacterium tumefaciens* using the floral dip method (Clough and Bent, 1998).

For *in vitro* biochemical analyses, the full-length *APC11* cDNA was amplified from Col-0 seedlings using RT-PCR, and ligated to

pGEX-6P-1 (GE, http://www3.gehealthcare.com/) and *pBI121-35S-nGFP* to make *p35S:GST-APC11* and *p35S:GFP-APC11*, respectively. The coding sequence of *cyclin B1;1* was amplified from Col-0 seedlings using RT-PCR and introduced to *pBI121-35S-6×cMyc* to make *p35S:CYCB1;1-Myc*. *CYCB1;1-4×Myc* was amplified from *pBI121-35S-CYCB1;1-6×cMyc* and ligated to pET48b(+) (Novagen, http://www.merckmillipore.com/) to generate *His-CYCB1;1-Myc* with a 4×Myc tag.

For phenotypic analyses of non-degradable *CYCB1;1*$^{\triangle D\text{-}box}$ transgenic plants, *cyclin B1;1* was introduced into *pEASY-Blunt* (TransGen, http://www.transgenbiotech.com/), and then the D-box RQVLGDIGN in cyclin B1;1 was mutated to AQVAGDIGN by PCR to make *pEASY-Blunt-CYCB1;1*$^{\triangle D\text{-}box}$. For embryo-specific expression (*pDD45:CYCB1;1-uidA*; *pDD45:CYCB1;1*$^{\triangle D\text{-}box}$*-uidA*), the PCR products of the 1020-bp *DD45* promoter and *CYCB1;1* or *CYCB1;1*$^{\triangle D\text{-}box}$ were inserted into *pGreen II*, with *uidA* fused in-frame. The primers used are listed in Table S2.

Microscopic and histological analyses

Ovules at different stages were cleared and observed as reported (Yu *et al.*, 2012). A confocal laser scanning microscope (FV1000MPE, Olympus, http://www.olympus-ims.com/) was used to examine *GFP* and *mCherry* expression in transgenic plants, with 488-nm and 543-nm excitation lasers, respectively. The GUS assay was performed as described (Xu *et al.*, 2005).

In vitro ubiquitination and degradation assays

In vitro ubiquitination assay was performed in a reaction consisting of 50 mM 2-amino-2-(hydroxymethyl)-1,3-propanediol (TRIS)/HCl (pH 7.4), 10 mM $MgCl_2$, 2 mM DTT, 5 mM ATP, a crude extract of recombinant 6×His-tagged wheat E1 (GI: 136632), 500 ng of purified 6×His-tagged human E2 (UBCh5b), 2 μg of 6×His-tagged ubiquitin and 0.5–1 μg purified APC11-GST as described (Zhao *et al.*, 2013). Divided mixtures were incubated at 24°C for 30, 60, 90 or 120 min, terminated by adding a loading buffer containing SDS, and boiled for 5 min before gel analysis. Proteins were detected by Western blot and visualized under the Chemiluminescent Imaging System (Tanon-5200, http://www.biotanon.com/).

For *in vitro* protein degradation assays, *A. tumefaciens* strains carrying *GFP-APC11*, *GFP* or *CYCB1;1-Myc* constructs were infiltrated to *N. benthamiana* leaves individually with *p19* at a 1:1 ratio (Voinnet *et al.*, 2003). Three days after infiltration, proteins were extracted using a native extraction buffer [50 mM TRIS-MES (pH 8.0), 0.5 M sucrose, 1 mM $MgCl_2$, 10 mM EDTA, 5 mM DTT and protease inhibitor cocktail tablets (Roche, http://www.roche.com/)] (Liu *et al.*, 2010). The CYCB1;1-Myc was mixed with GFP-APC11 or GFP in a volume ratio of 1:1. 10 μM ATP or 50 μM MG132 was added to the reaction mixture to promote or inhibit the 26S proteasome activity, respectively. DMSO at a final concentration of 50 μM was used as the negative control. These mixtures were incubated at room temperature (24°C) with gentle shaking at different time points for Western blot analyses.

ACCESSION NUMBERS

Sequence data from this article can be found in the EMBL/GenBank under the following accession numbers: *APC11* (*At3g05870*), *cyclin B1;1* (*At4g37490*), *APC1* (*At5g05560*), *APC4* (*At4g21530*), wheat *E1* (GI: 136632), human *E2* (*UBCh5b*, GI: 1216392), and Arabidopsis ubiquitin 14 (*At4g02890*). The T-DNA insertion line *zyg1-2*/+ used was SALK_019654. The correct annotation of *APC11* (*At3g05870*) has been submitted to GenBank with the accession number KT595418.

ACKNOWLEDGEMENTS

We thank Dr Ming Yang (Oklahoma State University) for critical comments, Dr Jingbo Jin for providing *pBI121-35S-6×cMyc* and *pBI121-35S-nGFP* constructs, Dr Lijia Qu for providing *apc1-1*/+ and *apc4-3*/+ seeds, and Dr Huaqin Gong and Mr Yongfeng Fan for technical support. This work is supported by the National Basic Research Program of China (2014CB943401; 2013CB967301) and the Sino-Dutch International Collaboration Project (31161130531).

AUTHOR CONTRIBUTIONS

LJ performed mutant screening, map-based cloning and basic expression analyses; LG performed extensive genetic, expression and biochemical analyses; YZ performed subcellular localization analyses during mitosis; XLL carried out some genetic analyses; CML guided the study; LG and LJ drafted the manuscript; and CML, QX and DW helped in designing experiments and revising the manuscript.

CONFLICT OF INTERESTS

The authors declare no competing financial interests.

SUPPORTING INFORMATION

Additional Supporting Information may be found in the online version of this article.

Figure S1. The genomic and cDNA sequences of *APC11*.

Table S1. Genetic analyses of embryo-lethal phenotypes in heterozygous *apc1-1*/+ and *apc4-3*/+ mutants.

Table S2. Primers used in this study.

REFERENCES

Andreuzza, S., Li, J., Guitton, A.E., Faure, J.E., Casanova, S., Park, J.S., Choi, Y., Chen, Z. and Berger, F. (2010) DNA LIGASE I exerts a maternal effect on seed development in *Arabidopsis thaliana*. *Development*, **137**, 73–81.

Autran, D., Baroux, C., Raissig, M.T. *et al.* (2011) Maternal epigenetic pathways control parental contributions to Arabidopsis early embryogenesis. *Cell*, **145**, 707–719.

Baroux, C., Autran, D., Gillmor, C.S., Grimanelli, D. and Grossniklaus, U. (2008) The maternal to zygotic transition in animals and plants. *Cold Spring Harb. Symp. Quant. Biol.* **73**, 89–100.

Blilou, I., Frugier, F., Folmer, S. *et al.* (2002) The Arabidopsis *HOBBIT* gene encodes a CDC27 homolog that links the plant cell cycle to progression of cell differentiation. *Genes Dev.* **16**, 2566–2575.

Boruc, J. and Van Damme, D. (2015) Endomembrane trafficking overarching cell plate formation. *Curr. Opin. Plant Biol.* **28**, 92–98.

Capron, A., Ökrész, L. and Genschik, P. (2003a) First glance at the plant APC/C, a highly conserved ubiquitin-protein ligase. *Trends Plant Sci.* **8**, 83–89.

Capron, A., Serralbo, O., Fülöp, K. *et al.* (2003b) The Arabidopsis anaphase-promoting complex or cyclosome: molecular and genetic characterization of the APC2 subunit. *Plant Cell*, **15**, 2370–2382.

Chang, L. and Barford, D. (2014) Insights into the anaphase-promoting complex: a molecular machine that regulates mitosis. *Curr. Opin. Struct. Biol.* **29**, 1–9.

Clough, S.J. and Bent, A.F. (1998) Floral dip: a simplified method for *Agrobacterium*-mediated transformation of *Arabidopsis thaliana*. *Plant J.* **16**, 735–743.

Colón-Carmona, A., You, R., Haimovitch-Gal, T. and Doerner, P. (1999) Spatio-temporal analysis of mitotic activity with a labile cyclin-GUS fusion protein. *Plant J.* **20**, 503–508.

De Rybel, B., van den Berg, W., Lokerse, A., Liao, C.Y., van Mourik, H., Möller, B., Peris, C.L. and Weijers, D. (2011) A versatile set of ligation-independent cloning vectors for functional studies in plants. *Plant Physiol.* **156**, 1292–1299.

De Smet, I., Lau, S., Mayer, U. and Jürgens, G. (2010) Embryogenesis – the humble beginnings of plant life. *Plant J.* **61**, 959–970.

Del Toro-De León, G., García-Aguilar, M. and Gillmor, C.S. (2014) Non-equivalent contributions of maternal and paternal genomes to early plant embryogenesis. *Nature*, **514**, 624–627.

Denninger, P., Bleckmann, A., Lausser, A. *et al.* (2014) Male-female communication triggers calcium signatures during fertilization in Arabidopsis. *Nat. Commun.* **5**, 4645.

Eloy, N.B., de Freitas Lima, M., Van Damme, D. *et al.* (2011) The APC/C subunit 10 plays an essential role in cell proliferation during leaf development. *Plant J.* **68**, 351–363.

Fülöp, K., Tarayre, S., Kelemen, Z. *et al.* (2005) Arabidopsis anaphase-promoting complexes: multiple activators and wide range of substrates might keep APC perpetually busy. *Cell Cycle*, **4**, 1084–1092.

Gmachl, M., Gieffers, C., Podtelejnikov, A.V., Mann, M. and Peters, J.M. (2000) The RING-H2 finger protein APC11 and the E2 enzyme UBC4 are sufficient to ubiquitinate substrates of the anaphase-promoting complex. *Proc. Natl Acad. Sci. USA*, **97**, 8973–8978.

Gray, W.M., Hellmann, H., Dharmasiri, S. and Estelle, M. (2002) Role of the Arabidopsis RING-H2 protein RBX1 in RUB modification and SCF function. *Plant Cell*, **14**, 2137–2144.

Guo, L. and Liu, C.M. (2015) A single-nucleotide exon found in Arabidopsis. *Sci. Rep.* **5**, 18087.

Gutierrez, R., Lindeboom, J.J., Paredez, A.R., Emons, A.M.C. and Ehrhardt, D.W. (2009) Arabidopsis cortical microtubules position cellulose synthase delivery to the plasma membrane and interact with cellulose synthase trafficking compartments. *Nat. Cell Biol.* **11**, 797–806.

Horner, V.L. and Wolfner, M.F. (2008) Transitioning from egg to embryo: triggers and mechanisms of egg activation. *Dev. Dyn.* **237**, 527–544.

Ingouff, M., Sakata, T., Li, J., Sprunck, S., Dresselhaus, T. and Berger, F. (2009) The two male gametes share equal ability to fertilize the egg cell in *Arabidopsis thaliana*. *Curr. Biol.* **19**, R19–R20.

Kwee, H.S. and Sundaresan, V. (2003) The *NOMEGA* gene required for female gametophyte development encodes the putative APC6/CDC16 component of the anaphase promoting complex in Arabidopsis. *Plant J.* **36**, 853–866.

Lechner, E., Xie, D., Grava, S. *et al.* (2002) The AtRbx1 protein is part of plant SCF complexes, and its down-regulation causes severe growth and developmental defects. *J. Biol. Chem.* **277**, 50069–50080.

Leverson, J.D., Joazeiro, C.A.P., Page, A.M., Huang, H., Hieter, P. and Hunter, T. (2000) The APC11 RING-H2 finger mediates E2-dependent ubiquitination. *Mol. Biol. Cell*, **11**, 2315–2325.

Li, H.J., Liu, N.Y., Shi, D.Q., Liu, J. and Yang, W.C. (2010) YAO is a nucleolar WD40-repeat protein critical for embryogenesis and gametogenesis in Arabidopsis. *BMC Plant Biol.* **10**, 169.

Lin, Z., Yin, K., Zhu, D., Chen, Z., Gu, H. and Qu, L.J. (2007) AtCDC5 regulates the G2 to M transition of the cell cycle and is critical for the function of Arabidopsis shoot apical meristem. *Cell Res.* **17**, 815–828.

Liu, L., Zhang, Y., Tang, S., Zhao, Q., Zhang, Z., Zhang, H., Dong, L., Guo, H. and Xie, Q. (2010) An efficient system to detect protein ubiquitination by agroinfiltration in *Nicotiana benthamiana*. *Plant J.* **61**, 893–903.

Meinke, D., Muralla, R., Sweeney, C. and Dickerman, A. (2008) Identifying essential genes in *Arabidopsis thaliana*. *Trends Plant Sci.* **13**, 483–491.

Müller, S. and Jürgens, G. (2015) Plant cytokinesis – no ring, no constriction but centrifugal construction of the partitioning membrane. *Semin. Cell Dev. Biol.* doi: 10.1016/j.semcdb.2015.10.037.

Nodine, M.D. and Bartel, D.P. (2012) Maternal and paternal genomes contribute equally to the transcriptome of early plant embryos. *Nature*, **482**, 94–97.

Pérez-Pérez, J.M., Serralbo, O., Vanstraelen, M., González, C., Criqui, M.C., Genschik, P., Kondorosi, E. and Scheres, B. (2008) Specialization of CDC27 function in the *Arabidopsis thaliana* anaphase-promoting complex (APC/C). *Plant J.* **53**, 78–89.

Peters, J.M. (2006) The anaphase promoting complex/cyclosome: a machine designed to destroy. *Nat. Rev. Mol. Cell Biol.* **7**, 644–656.

Raich, W.B., Moran, A.N., Rothman, J.H. and Hardin, J. (1998) Cytokinesis and midzone microtubule organization in *Caenorhabditis elegans* require the kinesin-like protein ZEN-4. *Mol. Biol. Cell*, **9**, 2037–2049.

Ronceret, A., Gadea-Vacas, J., Guilleminot, J., Lincker, F., Delorme, V., Lahmy, S., Pelletier, G., Chabouté, M.E. and Devic, M. (2008) The first zygotic division in Arabidopsis requires *de novo* transcription of thymidylate kinase. *Plant J.* **53**, 776–789.

Roodbarkelari, F., Bramsiepe, J., Weinl, C., Marquardt, S., Novák, B., Jakoby, M.J., Lechner, E., Genschik, P. and Schnittger, A. (2010) CULLIN 4-RING FINGER-LIGASE plays a key role in the control of endoreplication cycles in Arabidopsis trichomes. *Proc. Natl Acad. Sci. USA*, **107**, 15275–15280.

Saunders, C.M., Larman, M.G., Parrington, J., Cox, L.J., Royse, J., Blayner, L.M., Swann, K. and Lai, F.A. (2002) PLCζ: a sperm-specific trigger of Ca^{2+} oscillations in eggs and embryo development. *Development*, **129**, 3533–3544.

Schmidt, A., Duncan, P.I., Rauh, N.R., Sauer, G., Fry, A.M., Nigg, E.A. and Mayer, T.U. (2005) *Xenopus* polo-like kinase Plx1 regulates XErp1, a novel inhibitor of APC/C activity. *Genes Dev.* **19**, 502–513.

Sette, C., Bevilacqua, A., Bianchini, A., Mangia, F., Geremia, R. and Rossi, P. (1997) Parthenogenetic activation of mouse eggs by microinjection of a truncated c-kit tyrosine kinase present in spermatozoa. *Development*, **124**, 2267–2274.

Shen, W.H., Parmentier, Y., Hellmann, H. *et al.* (2002) Null mutation of *AtCUL1* causes arrest in early embryogenesis in Arabidopsis. *Mol. Biol. Cell*, **13**, 1916–1928.

Steffen, J.G., Kang, I.H., Macfarlane, J. and Drews, G.N. (2007) Identification of genes expressed in the Arabidopsis female gametophyte. *Plant J.* **51**, 281–292.

Tischer, T., Hörmanseder, E. and Mayer, T.U. (2012) The APC/C inhibitor XErp1/Emi2 is essential for *Xenopus* early embryonic divisions. *Science*, **338**, 520–524.

Tung, J.J., Hansen, D.V., Ban, K.H., Loktev, A.V., Summers, M.K., Adler, J.R. III and Jackson, P.K. (2005) A role for the anaphase-promoting complex inhibitor Emi2/XErp1, a homolog of early mitotic inhibitor 1, in cytostatic factor arrest of *Xenopus* eggs. *Proc. Natl Acad. Sci. USA*, **102**, 4318–4323.

Vielle-Calzada, J.P., Baskar, R. and Grossniklaus, U. (2000) Delayed activation of the paternal genome during seed development. *Nature*, **404**, 91–94.

Voinnet, O., Rivas, S., Mestre, P. and Baulcombe, D. (2003) An enhanced transient expression system in plants based on suppression of gene silencing by the p19 protein of tomato bushy stunt virus. *Plant J.* **33**, 949–956.

Wang, Y., Hou, Y., Gu, H., Kang, D., Chen, Z., Liu, J. and Qu, L.J. (2012) The Arabidopsis APC4 subunit of the anaphase-promoting complex/cyclosome (APC/C) is critical for both female gametogenesis and embryogenesis. *Plant J.* **69**, 227–240.

Wang, Y., Hou, Y., Gu, H., Kang, D., Chen, Z.L., Liu, J. and Qu, L.J. (2013) The Arabidopsis anaphase-promoting complex/cyclosome subunit 1 is critical for both female gametogenesis and embryogenesis. *J. Integr. Plant Biol.* **55**, 64–74.

Wassarman, P.M. (1987) The biology and chemistry of fertilization. *Science*, **235**, 553–560.

Weijers, D., Geldner, N., Offringa, R. and Jürgens, G. (2001) Seed development: early paternal gene activity in Arabidopsis. *Nature*, **414**, 709–710.

Weingartner, M., Criqui, M.C., Mészáros, T. *et al.* (2004) Expression of a nondegradable cyclin B1 affects plant development and leads to endomitosis by inhibiting the formation of a phragmoplast. *Plant Cell*, **16**, 643–657.

Wu, X., Viveiros, M.M., Eppig, J.J., Bai, Y., Fitzpatrick, S.L. and Matzuk, M.M. (2003) Zygote arrest 1 (*Zar1*) is a novel maternal-effect gene critical for the oocyte-to-embryo transition. *Nat. Genet.* **33**, 187–191.

Xu, J., Zhang, H.Y., Xie, C.H., Xue, H.W., Dijkhuis, P. and Liu, C.M. (2005) *EMBRYONIC FACTOR 1* encodes an AMP deaminase and is essential for the zygote to embryo transition in Arabidopsis. *Plant J.* **42**, 743–756.

Yu, D., Jiang, L., Gong, H. and Liu, C.M. (2012) *EMBRYONIC FACTOR 19* encodes a pentatricopeptide repeat protein that is essential for the initiation of zygotic embryogenesis in Arabidopsis. *J. Integr. Plant Biol.* **54**, 55–64.

Zhao, Q., Tian, M., Li, Q., Cui, F., Liu, L., Yin, B. and Xie, Q. (2013) A plant-specific *in vitro* ubiquitination analysis system. *Plant J.* **74**, 524–533.

Zheng, B., Chen, X. and McCormick, S. (2011) The anaphase-promoting complex is a dual integrator that regulates both microRNA-mediated transcriptional regulation of *Cyclin B1* and degradation of Cyclin B1 during Arabidopsis male gametophyte development. *Plant Cell*, **23**, 1033–1046.